

1. US EFFORT SUMMARY

1.1. Sandia – Justin L. Wagner

Efforts at Sandia National Laboratories have focused on fundamental experiments to understand the dispersal of dense particle distributions in high-speed compressible flow. The experiments are conducted in shock tube facilities where the flow conditions and the initial conditions of the particle distributions are well controlled and well characterized. An additional advantage of the shock tube is that it is more readily able to accommodate advanced measurement diagnostics in comparison to explosive field tests. Most experiments to date have taken place in the multiphase shock tube MST (Figure 1, left).

The method to generate a dense ‘particle curtain’ within the MST test section is as follows. Spherical particles rest on an initially closed gate valve, which is opened prior to firing the shock tube. The particles flow from a hopper into the test section before exiting through a slit in the floor (Figure 1, middle). The curtain flows for enough time to reach steady state prior to the arrival of the incident shock. The curtain spans the entire width of the test section with an isotropic distribution (Figure 1, right). The curtain typically has a streamwise-width δ_0 of 1.5 – 3 mm and a volume fraction residing between 3% and 23%. Experiments have used glass, steel, and tungsten spheres having diameters ranging from about 100 – 300 μm . Following the arrival of the incident shock wave at the curtain, a complex interaction occurs with the particles being dispersed in the high-speed compressible flow that follows the incident shock wave.

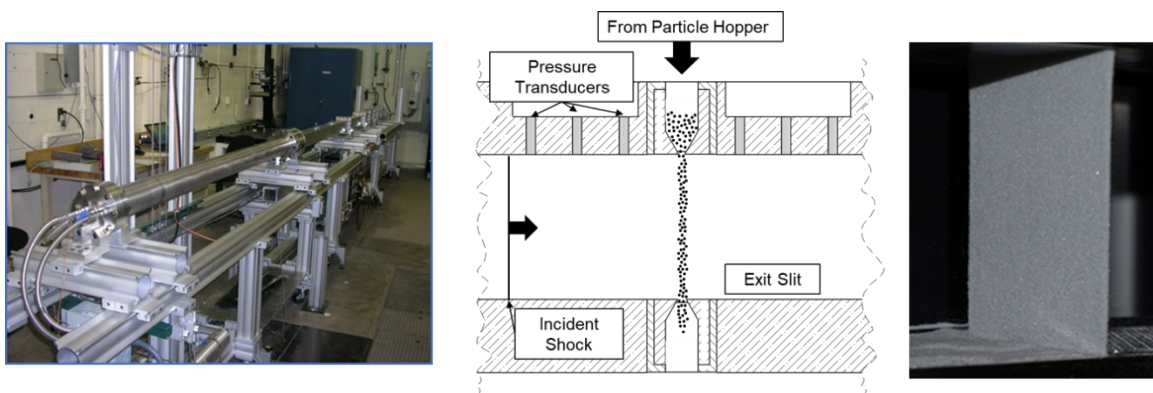


Figure 1 Photo of the multiphase shock tube MST (left), schematic showing the method to form a gravity-fed curtain with the MST test section (middle), and photo of the particle curtain (right) [1].

An example of particle dispersal following the arrival of the incident shock at the curtain is shown in Figure 2. In this experiment, the shock Mach number M_s is 1.40 and the curtain has a volume fraction at center-height of about 9%. Schlieren imaging at 75 kHz as well

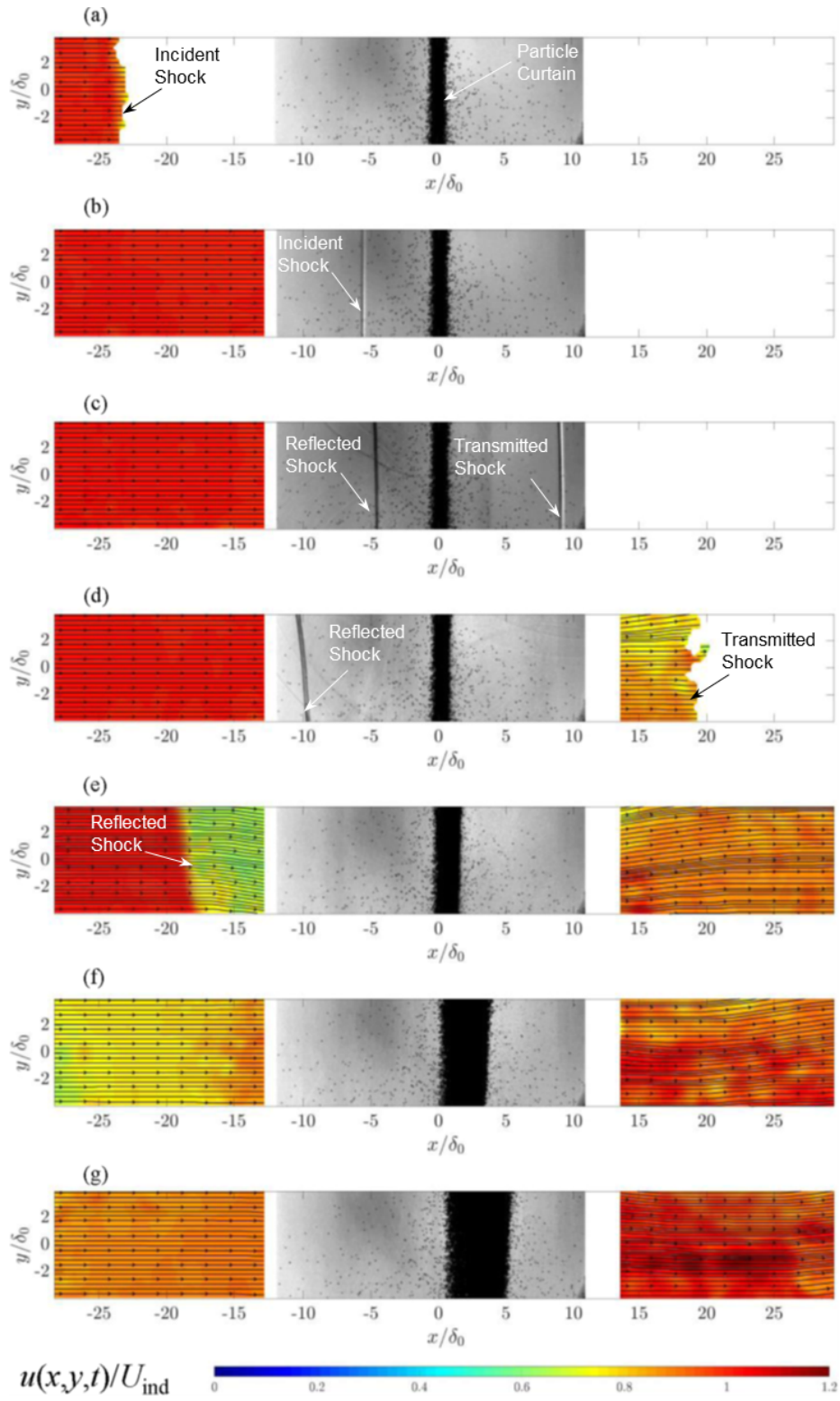


Figure 2 TR-PIV color contours of streamwise velocity with in-plane streamlines for $M_s = 1.40$, upstream and downstream of the particle curtain, with associated schlieren at $t^* =$ (a) -9.83 , (b) -2.27 , (c) 3.78 , (d) 8.31 , (e) $15.87, 27.96$, (g) 35.52 [2].

as time-resolved particle image velocimetry (TR-PIV) is utilized. The schlieren imaging is at the center of each subfigure, whereas contours of gas-phase velocity as returned by TR-PIV, straddle the schlieren upstream and downstream of the curtain. Here non-dimensional time $t^* = tU_{ind} / \delta_0$, where U_{ind} is equal to the velocity induced by the incident shock wave. In Figure 2a, the incident shock is observed near $x / \delta_0 = -25$. With continuing time (Figure 2b), the shock propagates into the schlieren field-of-view to just upstream of the particle curtain, which appears in shadow. Subsequently, in Figure 2c a transmitted and reflected shock are apparent. These shocks then move into the TR-PIV measurement regions (Figure 2d – Figure 2e). Finally, at later times, the curtain spreads at a noticeable rate and a high-speed turbulent flow is measured downstream of the curtain (Figure 2f – Figure 2g).

Predicting particle dispersal in high-speed flow requires detailed knowledge of the drag associated with dense particle clouds [3]. Data like those shown in Figure 2 can be used to measure the drag. Towards this end, a control volume analysis was performed to solve for the unsteady drag of the particle curtain using the TR-PIV data and concurrent fast-response pressure data [2]. An example result is shown Figure 3, which plots the drag coefficient C_D as a function of non-dimensional time. The time normalization is observed to collapse the data of varying shock Mach number, but two separate groupings appear that depend on the initial particle curtain volume fraction. This suggests that volume fraction plays an important role in particle dispersal.

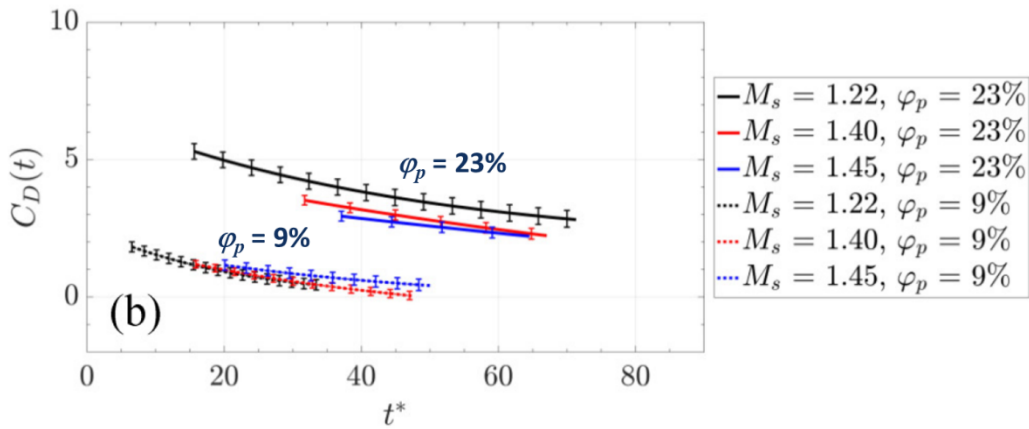


Figure 3 Drag coefficient as a function of non-dimensional time at shock Mach numbers ranging from 1.22 – 1.45 and and volume fractions φ from 9% - 23%. [2].

Although schlieren imaging is useful in tracking the particle curtain spread, it cannot be used in a quantitative fashion to measure the volume fraction distribution across the curtain. Flash X-ray radiography, on the other hand, can fill this gap with calibrated X-ray attenuation measurements. An example of volume fraction distributions during shock-

induced particle dispersal using this method is shown in Figure 4. Initially ($t^* = 0$), the curtain exhibits a Gaussian like distribution with a peak volume fraction near 23%. As the curtain spreads with time, the peak volume fraction decreases, and the profiles become skewed with higher volume fractions observed on the downstream front of the curtain. This effect is most pronounced in the $t^* = 35.5$ profile, which exhibits a sharp rise to peak, followed by a gradual fall.

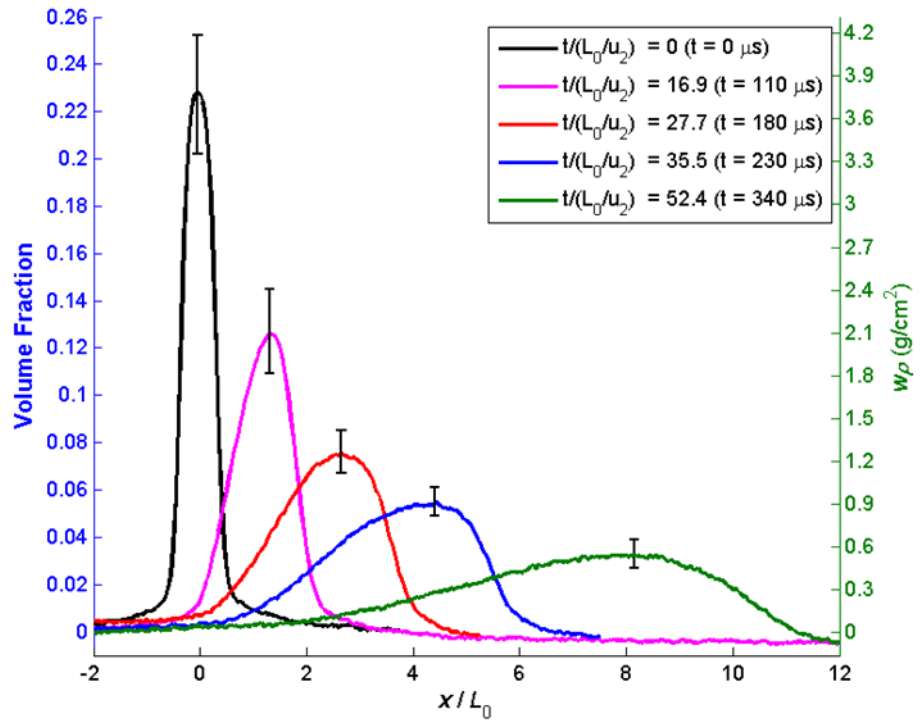


Figure 4 Volume fraction profiles obtained via flash X-ray during a $M_s = 1.67$ shock-particle curtain interaction [4].

The drag profiles in Figure 3 suggest the initial particle volume fraction of the curtain to be a critical parameter to momentum exchange between the high-speed gas and the particles. Recently, attempts to scale the spread of the particle curtain by a non-dimensional time have been made to further evaluate this hypothesis. An example is shown in Figure 5, where the thickness of the particle curtain in dimensional time (Figure 5a) is compared to that versus a non-dimensional time (Figure 5b) derived in DeMauro et al. [5]. The scaled time is a function of U_{ind} , δ_0 , and importantly, volume fraction. The scaled curtain spreads include data obtained in the Sandia experiments as well as those collected in other shock tubes where particles and initial curtain thicknesses are an order of magnitude larger. In all cases the particle material is soda lime glass. In Figure 5b, the particle diameter varies from about 100 – 1000 μm , δ_0 ranges from 1 – 30

mm, M_s ranges from 1.2 – 2.6, and the volume fraction goes from about 9 – 31%. Over this rather large range of parameters a strong collapse is observed.

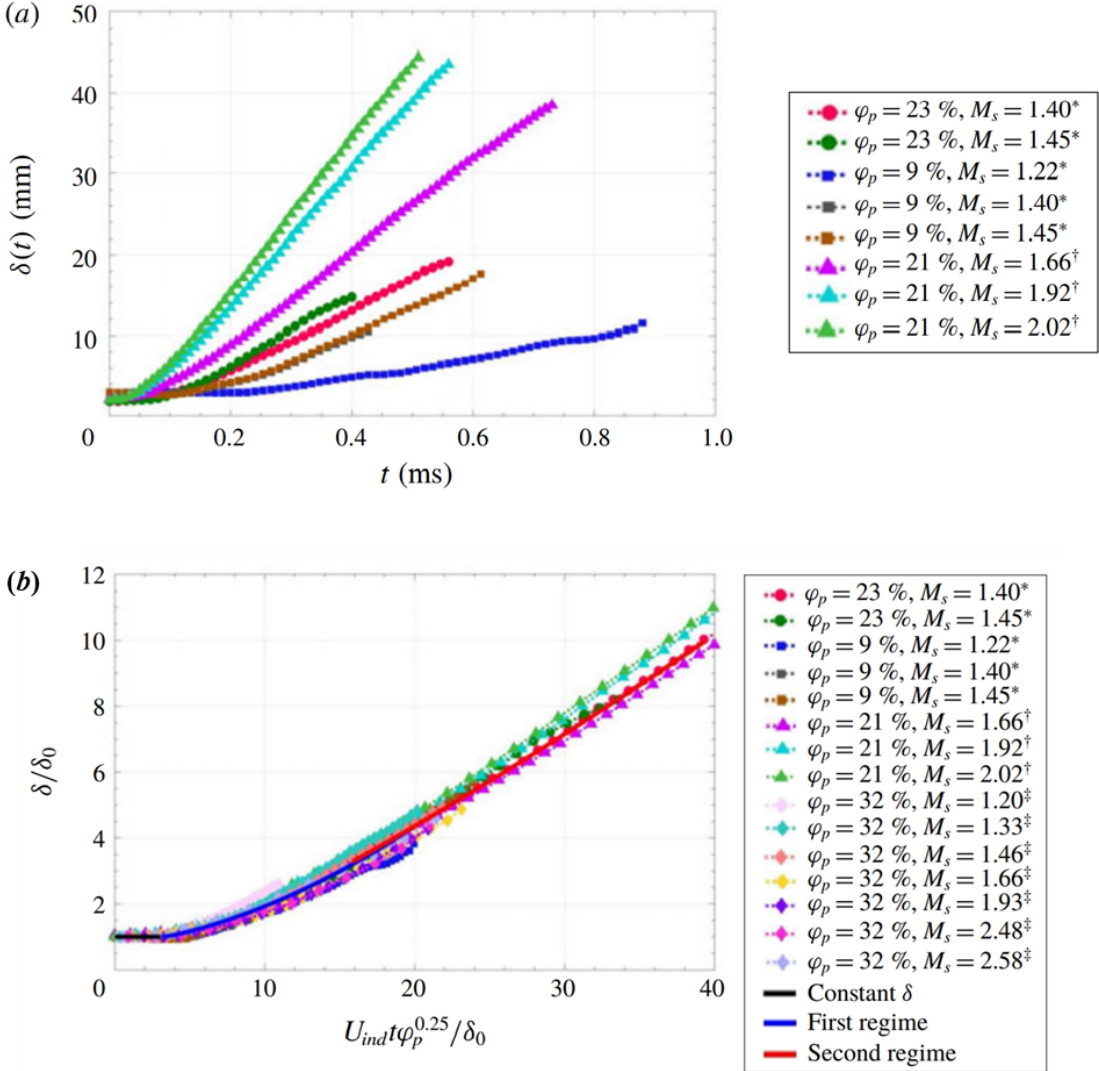


Figure 5 Normalized curtain thickness δ / δ_0 as function of dimensional (a) and non-dimensional time (b) [5]. All data correspond to particle curtains made of glass spheres.

The most recent experiments conducted at Sandia have focused on varying the particle curtain material to include stainless steel and tungsten spheres [6]. Unscaled data comparing the spread of these metal curtains to glass are shown in Figure 6a. For volume fractions above 17%, the tungsten curtain is observed to spread at a slower rate than the glass and steel, as expected. The DeMauro et al. [5] correlation also accounts for material density and is used to scale the data as shown in Figure 6b. The correlation does an excellent job collapsing the data, albeit at the modest shock Mach numbers tested to date.

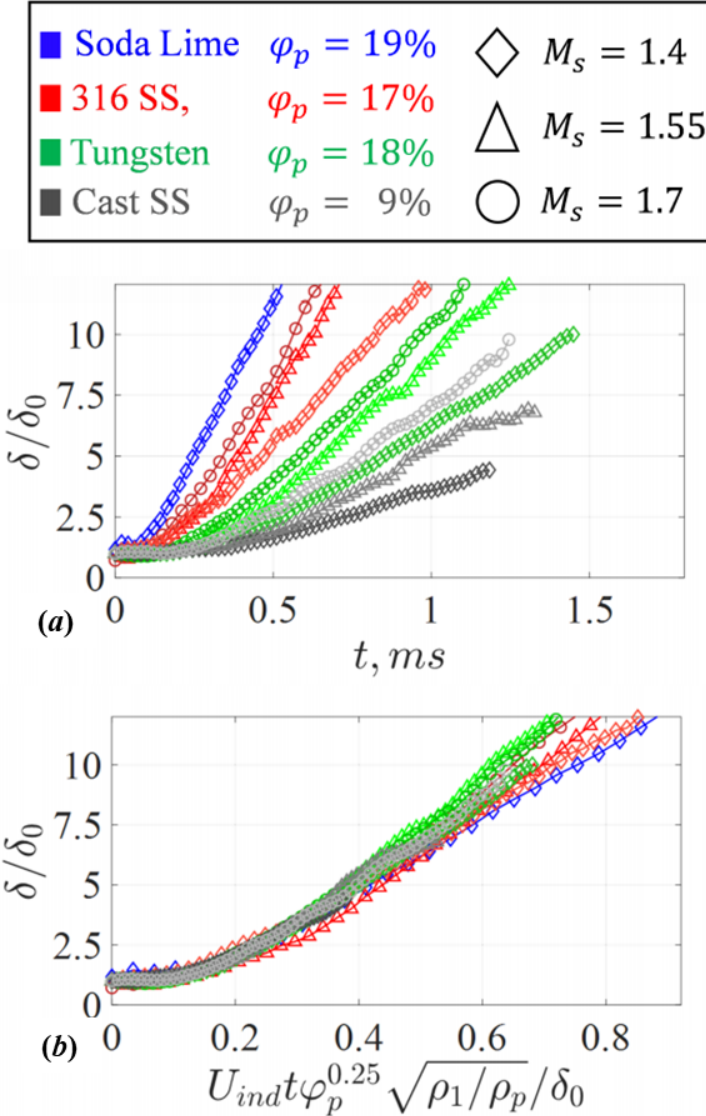


Figure 6 Normalized curtain thickness δ / δ_0 as function of dimensional (a) and non-dimensional time (b) [6]. Data include glass, steel and tungsten particle curtains.

Pushing the shock strength higher requires a methodology different than a standard shock tube such as the MST can provide. To create much stronger shock waves, a piston-driven facility denoted the high-temperature shock tube (HST) has been recently constructed. The HST can produce post-shock velocities > 1 km/s and post-shock temperatures greater than 2000 K [7]. Importantly, these conditions can be achieved using air initially at ambient atmospheric conditions as the test gas. A schematic of the HST is shown in Figure 7 and a detailed description can be found in Lynch et al. [7].

As described in Petter et al. [8], initial particle curtain experiments conducted in the HST produced qualitatively similar results to those in the MST. The HST, however, recoils during an experiment, which produces a ‘wavy’ undesirable initial curtain. Efforts are underway to mitigate this recoil by keeping the test section fixed. Additionally, experiments using reactive metal particle curtains will be conducted in the HST. These new experiments will be the subject of future publications.

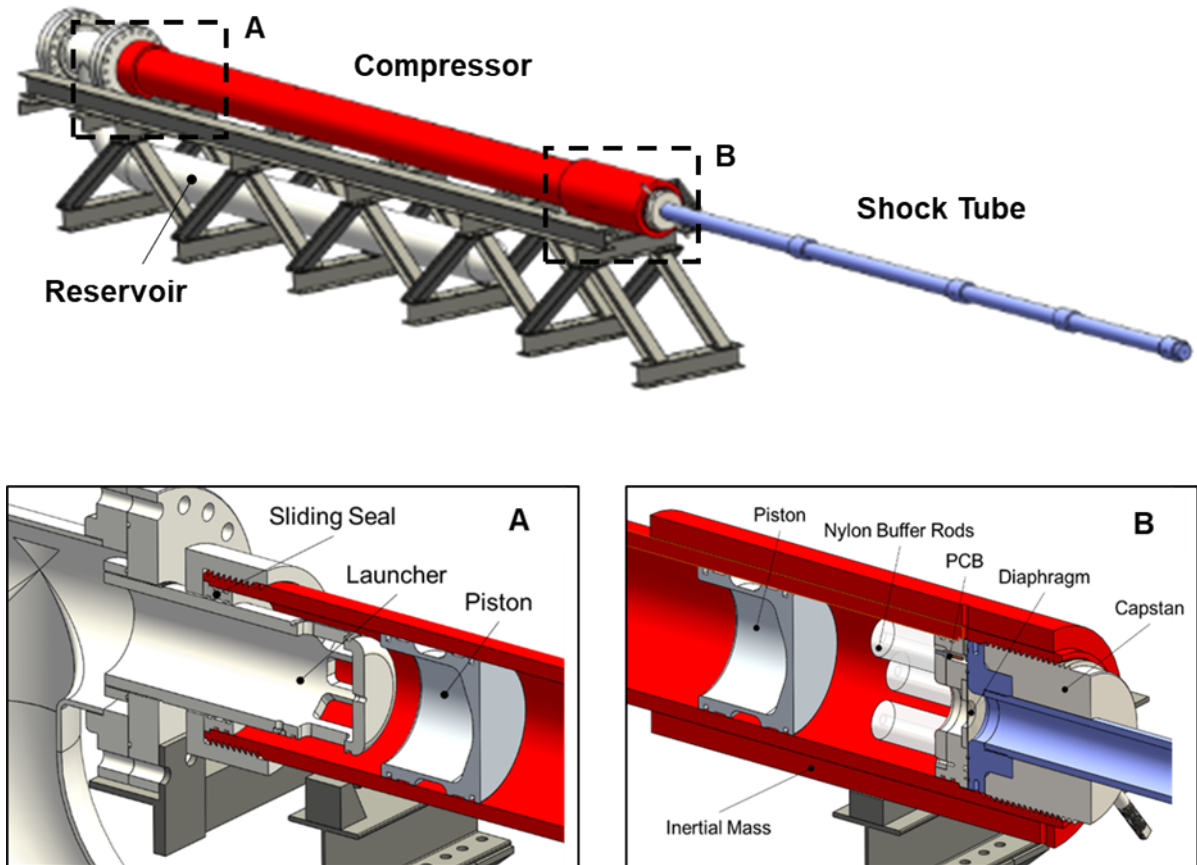


Figure 7 Schematic of the HST. A cutaway view of the launcher mechanism is shown in inset A and the diaphragm section is detailed in inset B.

APPENDIX A. BIBLIOGRAPHY

A.1.1. US:

1. Wagner, J.L., Beresh, S.J., Kearney, S.P., Trott, W.M., Castaneda, J.N., Pruett, B.O. and Baer, M.R. (2012). *A multiphase shock tube for shock wave interactions with dense particle fields*. Experiments in Fluids, 52(6), pp.1507-1517.
2. DeMauro, E.P., Wagner, J.L., Beresh, S.J. and Farias, P.A. (2017) *Unsteady drag following shock wave impingement on a dense particle curtain measured using pulse-burst PIV*. Physical Review Fluids, 2(6), p.064301.
3. Zhang, F., Frost, D.L., Thibault, P.A. and Murray, S.B. (2001) *Explosive dispersal of solid particles*. Shock Waves, 10(6), pp.431-443.
4. Wagner, J.L., Kearney, S.P., Beresh, S.J., DeMauro, E.P. and Pruett, B.O. (2015). *Flash X-ray measurements on the shock-induced dispersal of a dense particle curtain*. Experiments in Fluids, 56(12), pp.1-12.
5. DeMauro, E.P., Wagner, J.L., DeChant, L.J., Beresh, S.J. and Turpin, A.M. (2019). *Improved scaling laws for the shock-induced dispersal of a dense particle curtain*. Journal of Fluid Mechanics. 876, pp. 881-895
6. Daniel, K., Farias, P. and Wagner, J.L. (2021). *The shock-induced dispersal of dense particle curtains with varying density*. In AIAA Proc. Scitech 2021 Forum. AIAA 2021-0754.
7. Lynch, K. P., Spitzer, S., Grasser, T., Spillers, R., Farias, P. and Wagner, J. L., "A free-piston driven shock tube for generating extreme aerodynamic environments," In Proc. AIAA Scitech 2019, AIAA Paper 2019-1942.
8. Petter, S.J., Lynch, K.P., Farias, P., Spitzer, S., Grasser, T. and Wagner, J.L. (2020). *Early experiments on shock-particle interactions in the high-temperature shock tube*. In Proc. AIAA Scitech 2020 Forum, AIAA Paper 2020-0622.

Sandia National Laboratories is a multimission laboratory managed and operated by National Technology & Engineering Solutions of Sandia, LLC, a wholly owned subsidiary of Honeywell International Inc., for the U.S. Department of Energy's National Nuclear Security Administration under contract DE-NA0003525.



